

# Abnormal Distribution of Aquaporin-5 in Salivary Glands in the NOD Mouse Model for Sjögren's Syndrome

YRJÖ T. KONTTINEN, EVE-KAI TENSING, MIKAEL LAINE, PAULIINA POROLA, JYRKI TÖRNWALL, and MIKA HUKKANEN

**ABSTRACT. Objective.** To localize aquaporin-5 in healthy salivary gland acinar cells and to check if it is abnormally translocated in an experimental NOD mouse model for Sjögren's syndrome (SS).

**Methods.** Healthy BALB/c control mice and autoimmune focal adenitis NOD mice were studied. Aquaporin-5 was stained using avidin-biotin-peroxidase complex and indirect immunofluorescence staining methods, and visualized using light and laser scanning confocal microscopy.

**Results.** Aquaporin-5 was found in the apical domain of the acinar cell plasma membrane in healthy BALB/c mice. In contrast, aquaporin-5 was found in the apical and basolateral acinar plasma cell membrane in parotid, submandibular, and sublingual glands in NOD mice. This was confirmed using laser scanning confocal microscopy for optical sectioning and image reconstruction.

**Conclusion.** Our findings reveal an abnormal translocation of aquaporin-5 in an experimental SS animal model and support observations that implied a similar loss of the ordered and polarized expression of aquaporin-5 in human SS labial and lacrimal glands. (J Rheumatol 2005;32:1071–5)

*Key Indexing Terms:*

AQUAPORIN-5

NOD MOUSE

SJÖGREN'S SYNDROME

Sjögren's syndrome (SS) is an autoimmune exocrinopathy characterized by dry eyes and mouth combined with SS autoantibodies and focal sialadenitis<sup>1</sup>. Because the pathomechanisms responsible for diminished function of the exocrine glands are not known, a report that aquaporin-5 had lost its normal apical localization in secretory salivary acinar cells in SS patients raised considerable interest<sup>2</sup>. In SS patients aquaporin-5 was found to be diffusely distributed, not only in the apical, but also in the basolateral acinar plasma membrane domain. This finding on abnormal translocation was confirmed by Tsubota, *et al*, who reported

similar loss of acinar cell polarization in lacrimal glands<sup>3</sup>. However, a recent report seemed to refute these findings by describing what was interpreted as normal apical localization of aquaporin-5 in 5 SS patients<sup>4</sup>. In that report, laser scanning confocal microscopy was used and the authors claimed that this facilitated interpretation of the localization and, as stated above, that these findings refuted the 2 earlier articles. Inspired by this apparent discrepancy, we investigated this important topic using a new approach. We studied parotid, submandibular, and sublingual glands in a non-obese diabetic (NOD) mouse model for SS<sup>5,6</sup>, which is associated with salivary and lacrimal gland infiltrates, antinuclear antibodies, local tumor necrosis factor- $\alpha$  production, and progressively diminishing salivary and lacrimal flow rates. We used both immunoperoxidase and immunofluorescence labeling and laser scanning confocal microscopy. NOD mice were compared with healthy BALB/c control mice.

*From the Department of Medicine/Invärtes medicin, Helsinki University Central Hospital, ORTON Orthopaedic Hospital of the Invalid Foundation, Helsinki; COXA Hospital for Joint Replacement, Tampere; and Department of Anatomy, Institute of Biomedicine, University of Helsinki, Helsinki, Finland.*

*Supported by Finska Läkaresällskapet, HUS evo grant, Invalid Foundation, the Finnish Dental Society Apollonia, the Centre for International Mobility, and the University of Helsinki.*

*Y.T. Konttinen, MD, PhD, Department of Medicine/Invärtes medicin, Helsinki University Central Hospital, ORTON Orthopaedic Hospital of the Invalid Foundation, Helsinki, COXA Hospital for Joint Replacement, Tampere; E-K. Tensing, MD, Department of Medicine/Invärtes medicin, Helsinki University Central Hospital; M. Laine, DDS, Medical Student, Department of Anatomy, Institute of Biomedicine, University of Helsinki; P. Porola, BSc, Department of Anatomy, Institute of Biomedicine, University of Helsinki; J. Törnwall, MD, Department of Anatomy, Institute of Biomedicine, University of Helsinki; M. Hukkanen, PhD, Department of Anatomy, Institute of Biomedicine, University of Helsinki.*

*Address reprint requests to Prof. Y.T. Konttinen, Department of Medicine/invärtes medicin, Biomedicum, PO Box 700, Haartmaninkatu 8, FIN-00029 HUS, Finland. E-mail: yrjo.konttinen@helsinki.fi*

*Accepted for publication January 24, 2005.*

## MATERIALS AND METHODS

**Samples.** NOD mice (11 animals, age 20–26 weeks) and BALB/c mice (3 mice, 9 weeks old) were obtained from Scripps Research Institute (San Diego, CA, USA).

After killing the mice, parotid, submandibular, and sublingual salivary glands were fixed in 4% formalin. Fixed tissues were dehydrated in a series of graded ethanol solutions, immersed in xylene, and embedded in paraffin. Sections were cut at 3–4  $\mu$ m using a sliding microtome and then kept at 37°C overnight.

**Immunohistochemistry.** Deparaffinization of the samples was performed through xylene and graded ethanol solutions. For visualization of the antigen, a Vectastain Elite Rabbit IgG (Vector Laboratories, Burlingame, CA,

Personal non-commercial use only. The Journal of Rheumatology Copyright © 2005. All rights reserved.

USA) staining kit was used. Antigen retrieval was performed in 10 mM citric acid buffer, pH 6.0, for 24 min, using a Micromed T/T Mega microwave oven (Milestone Srl, Sorisole, Italy). Endogenous peroxidase was quenched in methanol with 0.3% of hydrogen peroxide for 30 min at room temperature. Slides were then incubated in 3% goat normal serum for 1 h at room temperature. Primary polyclonal rabbit IgG antibody against mouse aquaporin-5 (Alpha Diagnostic International, San Antonio, TX, USA) and negative control rabbit IgG (Jackson ImmunoResearch, West Grove, PA, USA) diluted in 0.1% bovine serum albumin in 10 mM phosphate buffered 0.15 M saline (PBS), pH 7.4, at concentration of 2 µg/ml were applied for overnight incubation at 4°C. This was followed by incubation in 1:100 diluted biotinylated secondary antibody for 1 h at room temperature and then avidin-biotin-peroxidase complex, which was prepared according to manufacturer's instructions, for 1 h at room temperature. Binding of avidin-biotin-peroxidase complex was visualized by applying a mixture of 3'3' diaminobenzamide tetrahydrochloride and hydrogen peroxide. Slides were counterstained with hematoxylin (Dako, Glostrup, Denmark).

Between steps (except between normal serum and primary antibody), slides were washed in 10 mM PBS, pH 7.4. All incubations took place in a humidified chamber. Specificity of primary antibody was controlled by preincubation with 10-fold excess of control peptide (Alpha Diagnostic International) for 1 h followed by use of antigen-preabsorbed primary antibody instead of the untreated primary antibody. Stained specimens were analyzed using a Leica microscope and a 12-bit cooled image SensiCam camera.

**Laser scanning confocal microscopy.** Three representative samples of both BALB/c and NOD mice were cut and sections deparaffinized through xylene and graded ethanol series. Antigen retrieval was done in 10 mM citrate buffer, pH 6, for 24 min using a microwave oven. Slides were then incubated in 3% goat normal serum (Dako) for 1 h at room temperature. Primary polyclonal rabbit IgG antibody against mouse aquaporin-5 (Alpha Diagnostic International) and negative control rabbit IgG (Jackson ImmunoResearch) diluted in 0.1% bovine serum albumin in PBS at concentration of 10 µg/ml were applied for overnight incubation at 4°C. Slides were incubated with 0.4 µg/ml fluorochrome conjugated goat anti-rabbit IgG (AlexaFluoro 488; Molecular Probes Inc., Eugene, OR, USA) for 1 h at room temperature. Nuclei were stained for 15 min with 1 µM TO-PRO-3 642/661 (Molecular Probes Inc.). Between steps, slides were washed with 10 mM phosphate buffered 0.15 M saline, pH 7.4, and coverslips were mounted using Vectashield (Vector).

Confocal microscopy was carried out using a Leica TCS SP2 system (Leica Microsystems AG, Wetzlar, Germany). Image stacks were collected through the specimen using a standardized sampling density of 160 nm. Selected image stacks were further subjected to deconvolution restoration using theoretical point-spread function and iterative maximum likelihood estimation algorithm (Scientific Volume Imaging BV, Hilversum, The Netherlands) before 3-dimensional image rendering with Imaris Surpass module (Bitplane AG, Zürich, Switzerland).

## RESULTS

**Healthy control mice.** Healthy BALB/c control mice displayed staining of the apical plasma membrane domain of the acinar cells in the parotid, submandibular, and sublingual glands (Figure 1, panels B, E, and H). This domain was facing the acinar lumen and extended some length down between the neighboring cells into the intercellular space. However, aquaporin-5 was not found in these normal glands in the basolateral plasma membrane domain of the acinar cells in any of the major salivary glands (Figure 1, panels B, E, and H). This basolateral plasma membrane domain was facing the basement membrane of the acinus and extended from there up between the neighboring cells into the intercellular space.

**NOD mice.** Diseased NOD mice with focal adenitis displayed staining of both the apical and basolateral plasma membrane domains of the acinar cells in the parotid, submandibular, and sublingual glands (Figure 1, panels A, D, and G). Thus, the polarized expression of aquaporin-5 was absent in focal sialadenitis in NOD mice.

**Laser scanning confocal imaging.** As 2-dimensional sections represent a simplified, flat view of a complex 3-dimensional tubuloalveolar gland, we stained 3 healthy and 3 disease samples also using immunofluorescence to visualize cell membrane localization of aquaporin-5 using laser scanning confocal microscopy. This allows scanning of tissue in different 3-dimensional planes and the figure stacks produced can then be combined using specific software. This method enabled us to confirm the apical restriction of aquaporin-5 in healthy BALB/c salivary glands and the loss of this restriction in diseased SS NOD salivary glands (Figure 2). In diseased NOD salivary glands, aquaporin-5 was found all around the acinar cells, on both the acinar and the basolateral plasma membrane.

**Staining controls.** Staining controls were performed for both immunoperoxidase and immunofluorescence staining. Antigen preabsorbed aquaporin-5-specific primary rabbit anti-human IgG antibodies were used at the same concentration as and instead of the primary antibodies. These results confirmed the specificity of immunohistochemical staining, as shown for immunoperoxidase in Figure 1, panels C, F, and I.

## DISCUSSION

Water molecules diffuse through intact lipid bilayer cell membranes very slowly. However, consistent with their exocrine secretory function, the apical cell membrane of the lacrimal and salivary gland acinar cells has highly permeable and water-selective channels, which increase its water permeability 10- to 100-fold. This water channel of the secretory glands is aquaporin-5. In acinar cells, water flow is regulated by osmotic and hydraulic gradients. Stimulation of the acinar cell opens an apical chloride channel, resulting in an accumulation of Cl<sup>-</sup> in the acinar lumen<sup>7</sup>. Positively charged Na<sup>+</sup> follows in order to preserve electroneutrality and the resulting osmotic gradient leads to water flow through aquaporin-5 channels. In addition, acini are embraced by ATPase- and myofilament-rich myoepithelial cells<sup>8</sup>. Their synchronous contraction squeezes the secretory endpiece to further stimulate the flow of water through aquaporin-5 channels. Roughly 10<sup>9</sup> H<sub>2</sub>O molecules in single file pass through aquaporin per second<sup>9</sup>. Therefore, the correct localization of aquaporin-5 to the apical cell membrane is important for correctly-directed secretory fluid flow. It has been established that the acinar aquaporin, aquaporin-5, is normally strictly restricted to the apical plasma membrane domain of the acinar cell<sup>10</sup>.

Tissue sections of parotid, submandibular, and sublingual

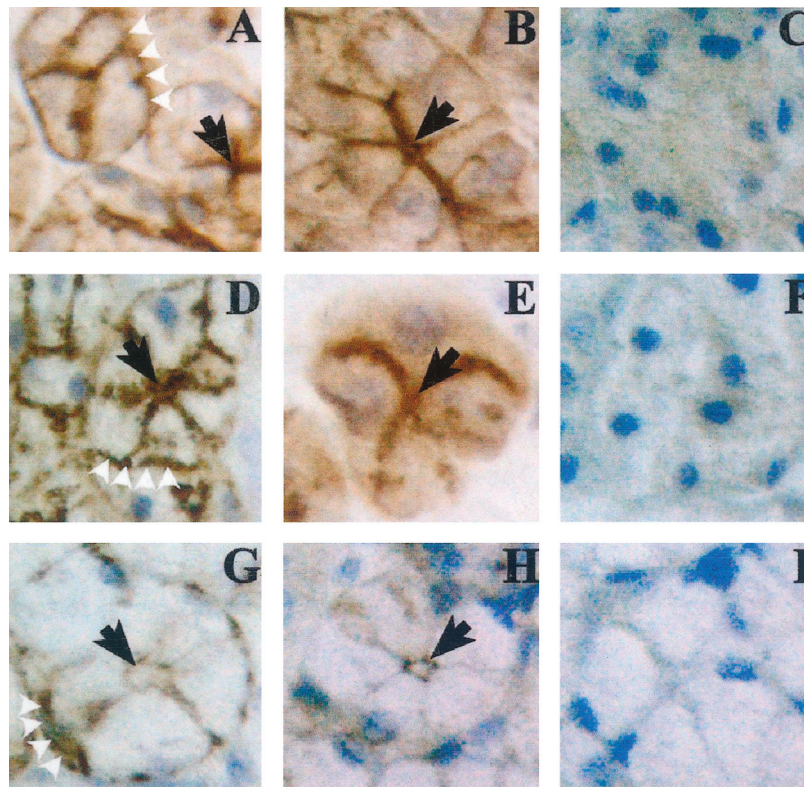


**Figure 1.** Aquaporin-5 in salivary glands in NOD and control mice. Note the immunoperoxidase staining of both the apical and the basolateral cell membrane domains in diseased NOD mice (A, D, G) compared to the apical restriction of aquaporin-5 in healthy BALB/c control mice (B, E, H) and negative staining controls (C, F, I). Panels A–C represent parotid, D–F submandibular, and G–I sublingual glands.

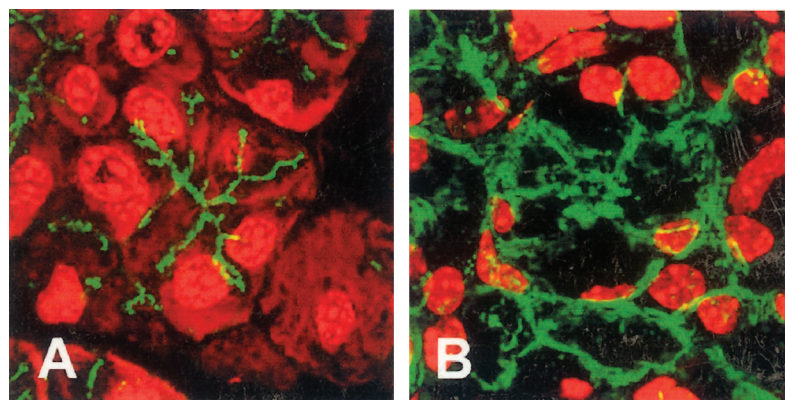


**Figure 2.** Aquaporin-5 in salivary glands in NOD and control mice. Representative optical sections produced using laser scanning confocal microscopy. A. BALB/c control gland with apical restriction of aquaporin-5. B. Diseased NOD glands with absent aquaporin-5 polarity and a typical staining pattern.

glands from healthy BALB/c control mice and NOD mice with focal adenitis were labeled with aquaporin-5-specific antibodies. Binding of these antibodies was visualized using avidin-biotin-peroxidase complex staining. All control mice had the characteristic apical localization. Aquaporin-5 lined the acinar lumen and extended from there in a centrifugal direction along the cell membrane, forming a star-like fig-

ure. Basolateral cell membrane did not stain. In contrast, in NOD mice in all 3 types of glands aquaporin-5 was not restricted to the apical cell membrane, but was also found along the basolateral cell membrane (Figure 1). Thus, aquaporin-5 had lost its cellular polarity.

To confirm these findings, 3 samples from each group were stained using indirect immunofluorescence and

inspected using laser scanning confocal microscopy. Again, healthy BALB/c controls were characterized by a star-like apically restricted aquaporin-5 pattern without staining of the basolateral plasma membrane domain, whereas diseased NOD glands were characterized by loss of the polarity of aquaporin-5 localization. Aquaporin-5 formed broad and intensely fluorescent bands on both the apical and basolateral cell membrane domains (Figure 2).

Our findings are in agreement with those published by Steinfeld, *et al*<sup>2</sup> and Tsubota, *et al*<sup>3</sup>. In contrast to Steinfeld, *et al*, Beroukas and coworkers<sup>4</sup> used laser scanning confocal microscopy in their salivary gland studies and did not observe abnormal location of aquaporin-5 in SS patients. We investigated this situation in a widely used experimental SS mouse model, employing 3 different types of glands, immunoperoxidase and immunofluorescence staining, and laser scanning confocal microscopy; we observed absent polarity of aquaporin-5 in NOD mice, whereas the healthy control mice were characterized by well established and normal apical restriction of aquaporin-5. Interpretation of 3-dimensional staining patterns from 2-dimensional sections is not necessarily easy. Laser scanning confocal microscopy allows optical sectioning and 3-dimensional reconstruction of acini in any spatial plane. Such 3-dimensional stacks clearly disclosed absent polarity of aquaporin-5 in NOD mouse salivary glands. Interestingly, Steinfeld, *et al* later published results on the use of infliximab, a tumor necrosis factor- $\alpha$  (TNF- $\alpha$ ) neutralizing chimeric antibody, in SS<sup>11</sup>. Apart from its small effect on various clinical disease indicators, this treatment also led to normalization of the aquaporin-5 staining pattern. Labial salivary glands in untreated patients were characterized by diffuse localization of aquaporin-5 on both apical and basolateral cell membrane, whereas the normal apical staining pattern was restored in post-treatment glands<sup>11</sup>. Since then, it has been shown in a large controlled clinical trial that infliximab is not effective in the treatment of SS<sup>12</sup>, but fortunately this interesting observation on the glandular effect of TNF- $\alpha$  blockade in SS had already been published<sup>11</sup>. This clearly demonstrates the difference between sialogogic stimuli, which do not affect aquaporin-5 distribution<sup>13</sup>, and stimuli associated with inflammation, such as locally produced TNF- $\alpha$ <sup>14</sup>. It has long been speculated that local TNF- $\alpha$  leads to a decreased response of the residual glandular cells to available neurotransmitters<sup>15,16</sup>. However, the mechanism responsible for this effect remains unknown. It now seems, based on work from several laboratories, that this is due to faulty translocation of aquaporin-5 as a result of TNF- $\alpha$ . Further, absent aquaporin-5 polarity in salivary glands was restored upon TNF- $\alpha$ -blocking inhibiting treatment<sup>11</sup>. We now extend these findings on human disease to the NOD mouse model. It can be argued that the NOD mouse is not a perfect model for SS, but it must be recognized that it shares some cardinal features with SS. For example, the NOD mouse devel-

ops spontaneous mononuclear cell infiltration of the salivary and lacrimal glands and antinuclear autoantibodies<sup>6</sup>. Histopathologically, the diseased exocrine glands display acinar cell atrophy and ductal epithelial cell hyperplasia associated with local production of TNF- $\alpha$ <sup>17</sup>. These changes are associated with increasing loss of salivary flow rates. We show that these changes are also associated with abnormal translocation of aquaporin-5 in the NOD mouse, findings that are compatible with those described in SS<sup>2,3</sup>. The main point is that both NOD mouse and SS patients have diminished salivary flow and that they also seem to share an abnormal aquaporin-5 translocation. Because laser scanning confocal microscopy is somewhat tedious compared with conventional microscopy, one possible reason for the apparent discrepancy between the salivary gland findings reported by Steinfeld, *et al*<sup>2</sup>, Tsubota, *et al*<sup>3</sup>, and ourselves compared to Beroukas, *et al*<sup>4</sup> could be field and sample selection bias, as only 5 patients with SS were investigated in the latter study.

## REFERENCES

1. Vitali C, Bombardieri S, Moutsopoulos HM, et al. Preliminary criteria for the classification of Sjögren's syndrome. Results of a prospective concerted action supported by the European Community. *Arthritis Rheum* 1993;36:340-7.
2. Steinfeld S, Cogan E, King LS, Agre P, Kiss R, Delporte C. Abnormal distribution of aquaporin-5 water channel protein in salivary glands from Sjögren's syndrome patients. *Lab Invest* 2001;81:143-8.
3. Tsubota K, Hirai S, King LS, Agre P, Ishida N. Defective cellular trafficking of lacrimal gland aquaporin-5 in Sjögren's syndrome. *Lancet* 2001;357:688-9.
4. Beroukas D, Hiscock J, Jonsson R, Waterman SA, Gordon TP. Subcellular distribution of aquaporin 5 in salivary glands in primary Sjögren's syndrome. *Lancet* 2001;358:1875-6.
5. Humphreys-Beher MG, Hu Y, Nakagawa Y, Wang PL, Purushotham KR. Utilization of the non-obese diabetic (NOD) mouse as an animal model for the study of secondary Sjögren's syndrome. *Adv Exp Med Biol* 1994;350:631-6.
6. Hu Y, Nakagawa Y, Purushotham KR, Humphreys-Beher MG. Functional changes in salivary glands of autoimmune disease-prone NOD mice. *Am J Physiol* 1992;263:E607-14.
7. Melvin JE, Kawaguchi M, Baum BJ, Turner RJ. A muscarinic agonist-stimulated chloride efflux pathway is associated with fluid secretion in rat parotid acinar cells. *Biochem Biophys Res Commun* 1987;145:754-9.
8. Pinkstaff CA. Cytology, histology, and histochemistry of salivary glands: an overview. In: Dobrosielski-Vergona K, editor. *Biology of the salivary glands*. Boca Raton, LA: CRC Press; 1993:30-1.
9. Zeidel ML, Ambudkar SV, Smith BL, Agre P. Reconstitution of functional water channels in liposomes containing purified red cell CHIP28 protein. *Biochemistry* 1992;31:7436-40.
10. Nielsen S, King LS, Christensen BM, Agre P. Aquaporins in complex tissues. II. Subcellular distribution in respiratory and glandular tissues of rat. *Am J Physiol* 1997;273:C1549-61.
11. Steinfeld SD, Appelboom T, Delporte C. Treatment with infliximab restores normal aquaporin 5 distribution in minor salivary glands of patients with Sjögren's syndrome. *Arthritis Rheum* 2002;46:2249-51.
12. Mariette X, Ravaud P, Steinfeld S, et al. Inefficacy of infliximab in primary Sjögren's syndrome: results of the randomized, controlled

- Trial of Remicade in Primary Sjögren's Syndrome (TRIPSS).  
*Arthritis Rheum* 2004;50:1270-6.
13. Gresz V, Kwon TH, Gong H, et al. Immunolocalization of AQP-5 in rat parotid and submandibular salivary glands after stimulation or inhibition of secretion in vivo. *Am J Physiol Gastrointest Liver Physiol* 2004;287:G151-61.
  14. Koski H, Janin A, Humphreys-Beher MG, Sorsa T, Malmstrom M, Kontinen YT. Tumor necrosis factor-alpha and receptors for it in labial salivary glands in Sjögren's syndrome. *Clin Exp Rheumatol* 2001;19:131-7.
  15. Fox RI, Stern M. Sjögren's syndrome: mechanisms of pathogenesis involve interaction of immune and neurosecretory systems. *Scand J Rheumatol* 2002;116 Suppl:3-13.
  16. Zhu Z, Stevenson D, Schechter JE, et al. Tumor necrosis factor inhibitor gene expression suppresses lacrimal gland immunopathology in a rabbit model of autoimmune dacryoadenitis. *Cornea* 2003;22:343-51.
  17. Takahashi M, Mimura Y, Hamano H, Haneji N, Yanagi K, Hayashi Y. Mechanism of the development of autoimmune dacryodenitis in the mouse model for primary Sjögren's syndrome. *Cell Immunol* 1996;170:54-62.